LETTERS

Five-dimensional optical recording mediated by surface plasmons in gold nanorods

Peter Zijlstra[1], James W. M. Chon[1] & Min Gu[1]

Multiplexed optical recording provides an unparalleled approach to increasing the information density beyond 10^{12} bits per cm^3 (1 Tbit cm^{-3}) by storing multiple, individually addressable patterns within the same recording volume. Although wavelength[1–3], polarization[4–8] and spatial dimensions[9–13] have all been exploited for multiplexing, these approaches have never been integrated into a single technique that could ultimately increase the information capacity by orders of magnitude. The major hurdle is the lack of a suitable recording medium that is extremely selective in the domains of wavelength and polarization and in the three spatial domains, so as to provide orthogonality in all five dimensions. Here we show true five-dimensional optical recording by exploiting the unique properties of the longitudinal surface plasmon resonance (SPR) of gold nanorods. The longitudinal SPR exhibits an excellent wavelength and polarization sensitivity, whereas the distinct energy threshold required for the photothermal recording mechanism provides the axial selectivity. The recordings were detected using longitudinal SPR-mediated two-photon luminescence, which we demonstrate to possess an enhanced wavelength and angular selectivity compared to conventional linear detection mechanisms. Combined with the high cross-section of two-photon luminescence, this enabled non-destructive, crosstalk-free readout. This technique can be immediately applied to optical patterning, encryption and data storage, where higher data densities are pursued.

The concept of five-dimensional patterning is illustrated in Fig. 1. The sample consists of a multilayered stack in which thin recording layers ($\sim1\,\mu m$) are separated by a transparent spacer ($\sim10\,\mu m$). In both the wavelength and polarization domains, three-state multiplexing is illustrated to provide a total of nine multiplexed states in one recording layer. The key to successfully realizing such five-dimensional encoding is a recording material that (1) is orthogonal in all dimensions, in both recording and readout, (2) is able to provide multiple recording channels in each dimension, and (3) is stable in ambient conditions and can be read out non-destructively. Existing multiplexing techniques[1–8] are only orthogonal in one dimension (either wavelength or polarization), and often ambient conditions and readout degrades the recorded patterns through unwanted isomerization or photobleaching.

We show that a recording material based on plasmonic gold nanorods meets all the above criteria. Gold nanorods have been extensively used in a wide range of applications because of their unique optical and photothermal properties. The narrow longitudinal SPR linewidth of a gold nanorod (100–150 meV, or ~45–65 nm in the near-infrared[14,15]; Supplementary Fig. 1), combined with the dipolar optical response, allows us to optically address only a small subpopulation of nanorods in the laser irradiated region. We use this selectivity to achieve longitudinal SPR mediated recording and readout governed by photothermal reshaping and two-photon luminescence (TPL) detection, respectively.
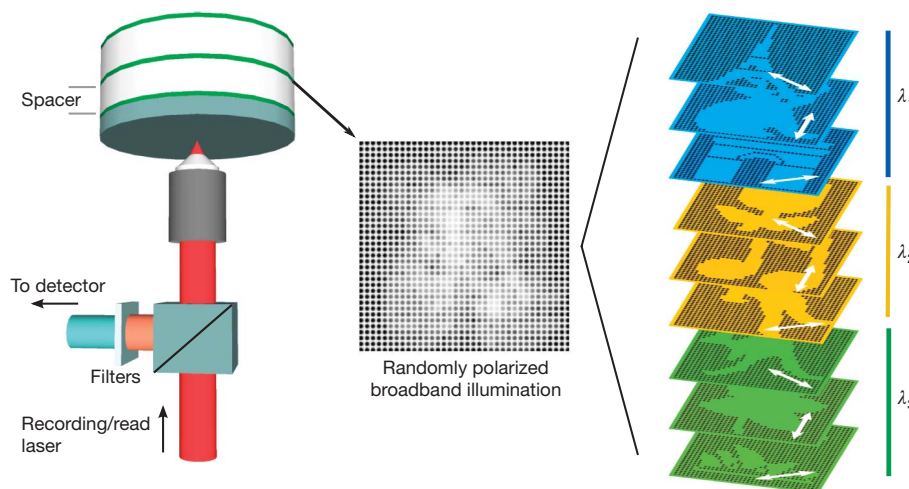
Figure 1 | Sample structure and patterning. Left, the sample consists of thin recording layers of spin-coated polyvinyl alcohol doped with gold nanorods, on a glass substrate. These recording layers were spaced by a transparent pressure-sensitive adhesive with a thickness of 10 μm. In the recording layers, we patterned multiple images using different wavelengths ($\lambda_{1–3}$) and polarizations of the recording laser. Middle, when illuminated with unpolarized broadband illumination, a convolution of all patterns will be observed on the detector (filters attenuate the reflected readout laser light). Right, when the right polarization and wavelength is chosen, the patterns can be read out individually without crosstalk.

[1]Centre for Micro-Photonics, Faculty of Engineering and Industrial Sciences, Swinburne University of Technology, PO Box 218, Hawthorn, Victoria 3122, Australia.

During recording, the absorption of a laser pulse induces a temperature rise in the selected nanorods. For sufficiently high laser pulse energy, the selected nanorods will heat up to above the threshold melting temperature, and transform their shape into shorter rods or spherical particles[16,17]. This results in a depleted population of nanorods with a certain aspect ratio and orientation (Fig. 2a), and hence a polarization dependent bleaching occurs in the extinction profile (Supplementary Fig. 2). Despite the single photon excitation of the longitudinal SPR, the threshold of the photothermal melting confines the writing process axially to within the focal volume and provides the ability to record three-dimensionally. This is in stark contrast to single photon recording by photobleaching or photo-isomerization, where the out-of-focus laser light would still induce recording.

In Fig. 2b we show the transmission electron microscope images and the extinction profiles of the three distributions of gold nanorods that we used in the recording layers. To confirm the selective reshaping, a mixture of the gold nanorods depicted in Fig. 2b was spin-coated on a glass coverslip. We acquired scanning electron microscope (SEM) images before (Fig. 2c) and after (Fig. 2d) irradiation with a single, linearly polarized femtosecond laser pulse ($\lambda = 840$ nm and pulse energy 0.28 nJ in the focal plane of the objective). We find that only nanorods with an aspect ratio of 3.4 ± 0.9 within an angular range of $25°$ with respect to the horizontal laser light polarization were affected by the laser pulse (averaged over 20 reshaped particles). Some of the rods were propelled from the glass interface owing to a rapid change in the centre of mass during the melting process, which was observed previously for gold triangles[18]. Such lift-off is prevented in our recording medium, as the nanorods are embedded in a thick polymer layer (Supplementary Fig. 3).

We imaged the recordings using longitudinal SPR mediated TPL. Previous reports on patterning in gold nanoparticles all used linear detection processes based on scattering[2] or extinction[5–7,19,20]. However, a nonlinear detection process such as TPL has a significantly higher angular and wavelength sensitivity. To demonstrate this, we acquired the scattering and TPL excitation profiles of a single gold nanorod (average aspect ratio 3, average size 90×30 nm) as a function of both wavelength and polarization (Fig. 3a and b). The nonlinear character of the TPL induces an excitation profile linewidth that is almost 60% narrower than the linewidth of the linear scattering spectrum (Fig. 3a, Supplementary Fig. 4). Furthermore, we find a reduction of almost 50% in the width of the angular excitation profile (Fig. 3b), which is in good agreement with previous observations[21,22]. The observed narrowing of the spectral and angular excitation profiles significantly reduces interference in the readout between neighbouring recording channels. Even more so, the axial sectioning induced by two-photon excitation allows for crosstalk-free readout of closely spaced layers. The most fascinating property of TPL is that it is most efficiently excited on resonance with the linear plasmon absorption band[21,22], enabling single photon recording and multi-photon readout using one and the same wavelength.

The TPL brightness of gold nanorods was characterized by calculating their TPL action cross-section ($=\eta\sigma_2$, where η is the luminescence quantum yield and σ_2 is the two-photon absorption cross-section) of a single gold nanorod following the method of ref. 23. From a TPL raster scan of isolated gold nanorods (average aspect ratio 4, average size 44×12 nm), we estimate the TPL action cross-section to be $\sim 3 \times 10^4$ GM (Göppert-Mayer) for excitation on resonance with the longitudinal SPR (for more details, see Supplementary Information page 6). From the TPL action cross-section, σ_2 can be calculated if η is known. Previous reports on photoluminescence of gold nanoparticles[24–26] suggest that the quantum yield of the nanorod geometry is drastically increased compared to spherical particles[25] or films[27]. The so-called 'lightning rod effect' around a nanorod is known to enhance the local field strength and the radiative decay rate via coupling to the SPR, and has been used to explain the observed increase in quantum yield from 10^{-10} for a film to $\sim 10^{-4}$ for rods with a size and aspect ratio similar to the ones studied here[24]. Assuming the reported quantum yield, we estimate that σ_2 is $\sim 3 \times 10^8$ GM. This is to our knowledge the highest σ_2 ever observed, with the previous highest report being 3.5×10^6 GM for a 4-nm gold nanoparticle[26]. We propose that this drastic increase is caused by the two orders of magnitude larger volume and intrinsically higher optical cross-section of our nanorods compared to the 4-nm-diameter gold nanoparticles used in ref. 26. The current direct measurement of the TPL action cross-section is also one order of magnitude larger than the value of 2.3×10^3 GM reported in ref. 21, which was indirectly determined by comparing the brightness of a single rhodamine 6G
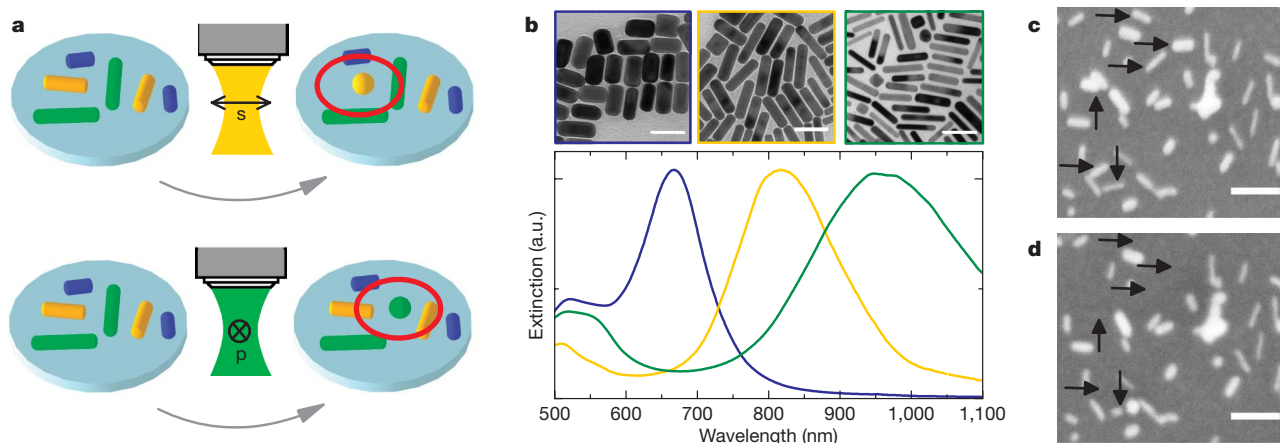
Figure 2 | Photothermal patterning. a, A schematic illustration of the patterning mechanism. The patterning is governed by photothermal reshaping of the gold nanorods in the focal volume of the focusing objective; this reshaping is selective in terms of aspect ratio and orientation. A linear polarized laser pulse will only be absorbed by gold nanorods that are aligned to the laser light polarization and which exhibit an absorption cross-section that matches the laser wavelength. Top, s-polarized laser light with a wavelength of 840 nm will only affect the nanorods with an intermediate aspect ratio that are aligned to the laser polarization (the reshaped rod is indicated). Bottom, p-polarized laser light with a wavelength of 980 nm only reshapes the high-aspect-ratio gold nanorods aligned to the laser light polarization (reshaped rod is indicated). **b**, Normalized extinction spectra of the as-prepared gold nanorod solutions. a.u., arbitrary units. Insets show transmission electron micrographs of the gold nanorods on a copper grid. The average sizes of the nanorods are, from left to right, 37×19 nm (aspect ratio 2 ± 1), 50×12 nm (aspect ratio 4.2 ± 1), and 50×8 nm (aspect ratio 6 ± 2). Scale bars, 50 nm. Each recording layer in the multi-layered sample is doped with a mixture of these gold nanorods to form an inhomogeneously broadened extinction profile. **c, d**, SEM images of gold nanorods spin-coated on an indium tin oxide coated glass coverslip before (**c**) and after (**d**) irradiation with a single femtosecond laser pulse of 840 nm with horizontal polarization. Rods affected by the laser pulse are arrowed. Scale bars, 100 nm.

Figure 3 | Readout using two-photon luminescence. a, Normalized white light scattering spectrum (red solid line) and two-photon luminescence (TPL) excitation profile (green circles) as a function of photon energy $\hbar\omega$ for individual gold nanorods with approximate dimensions of 90×30 nm. The profiles were centred around the longitudinal SPR energy $\hbar\Omega_{LSP}$. **b**, Polarized scattering (open squares) and TPL intensity (filled circles) versus the polarization of the excitation light. **c**, Normalized TPL raster scan of an image patterned using single laser pulses per pixel with a wavelength of 840 nm and vertical polarization. (Panels **c**–**f** are labelled with laser wavelength and a double-headed arrow indicating polarization direction.) The TPL was excited with the same wavelength and polarization as was used for the patterning. The pattern is 75×75 pixels, with a pixel spacing of 1.33 μm. Inset, high magnification image of the recording (size 7×7 μm). **d**–**f**, Images obtained when the TPL is excited at 840 nm with horizontal polarization (**d**), at 710 nm with vertical polarization (**e**), and at 980 nm with vertical polarization (**f**). Scale bars, 20 μm.

molecule to a single gold nanorod. The large TPL action cross-section allows us to non-destructively image the recordings by using very low excitation powers.

To illustrate the readout using TPL, we first recorded a single image using vertically polarized laser light with a wavelength of 840 nm (Fig. 3c). Pixels were written using a single femtosecond laser pulse focused through a 0.95 NA objective lens. Using single laser pulses per pixel prevents adverse accumulative thermal effects on the matrix, which were observed when a high repetition rate pulse train

was employed[20]. The recorded pattern was retrieved by raster scanning the sample and detecting the TPL signal from the gold nanorods. The TPL was excited with the same wavelength and polarization that was used for the patterning. The pixels exhibit a lower TPL signal owing to a depleted population of nanorods with a longitudinal SPR on resonance with the readout laser light. After deconvolution with the response function of the imaging objective, we find an average pixel size of 500 ± 100 nm, which is in good agreement with the expected diffraction limit of 470 nm. Because all the rods on resonance with the laser light were reshaped, the contrast of the pixels (defined as $|I_{pixel} - I_{bg}|/(I_{pixel} + I_{bg})$, with I_{pixel} and I_{bg} the pixel and background TPL signal, respectively) was 1. When this image was read in transmission mode, the contrast was found to be 0.05. Considering the nanorod concentration (Methods), we estimate that this contrast arises from the reshaping of ~30 nanorods in the focal volume. We do not observe any contrast when the TPL is excited with a horizontally polarized laser beam (Fig. 3d) or when the wavelength is tuned to 700 nm or 980 nm (Fig. 3e and f). This indicates that only the subpopulation of nanorods with a longitudinal SPR on resonance with the recording laser light has reshaped.

Using the longitudinal SPR mediated recording and readout mechanisms, we achieved for the first time five-dimensional optical recording. In Fig. 4 we show TPL raster scans of 18 images, all patterned in the same area. The patterning was conducted using a single femtosecond laser pulse per pixel at wavelengths of 700 nm, 840 nm and
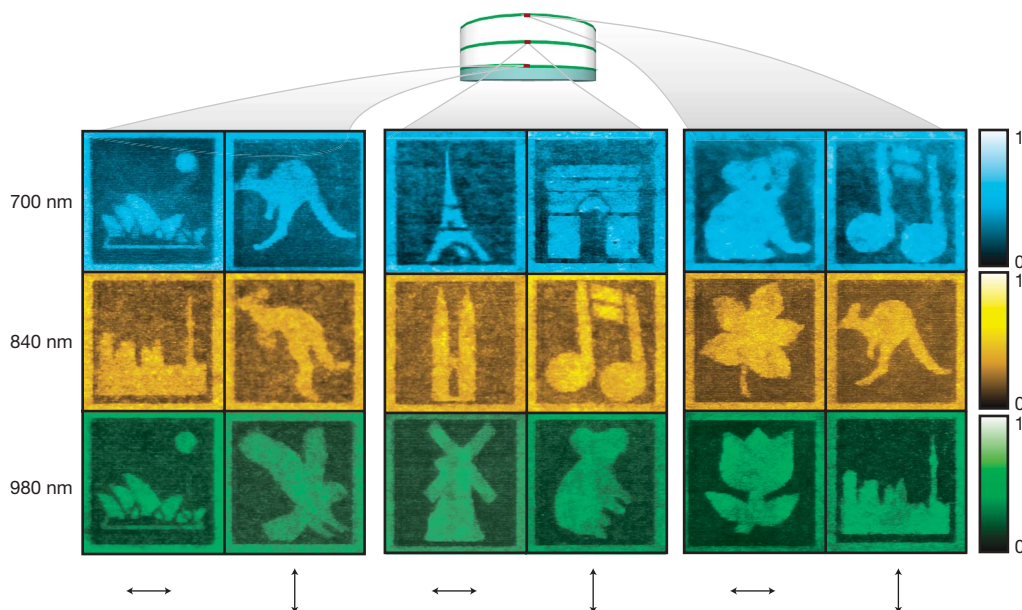
Figure 4 | Five-dimensional patterning and readout. Normalized TPL raster scans of 18 patterns encoded in the same area using two laser light polarizations and three different laser wavelengths. Patterns were written in three layers spaced by 10 μm. The recording laser pulse properties are indicated (wavelength at left, polarization at bottom). The recordings were retrieved by detecting the TPL excited with the same wavelength and polarization as employed for the recording. The size of all images is 100×100 μm, and the patterns are 75×75 pixels.

980 nm, with both horizontal and vertical polarization (see Methods for more details). Images were patterned in three layers, with a layer spacing of 10 µm and a bit spacing of 1.33 µm. The laser pulse energy and wavelength used for patterning were optimized to minimize crosstalk between the different recording channels. Although we used a femtosecond pulse laser for patterning, the recording can also be performed with a continuous wave laser or laser diode, paving the way for a low-cost recording apparatus (Supplementary Fig. 5).

Using this technique, improved security imprinting and encryption can be realized, where the added dimensions can act as an extended and counterfeit-proof encryption key. In such applications, it would be highly beneficial to have immediate access to the patterns without the need for raster scanning. In order to test this, we have recorded polarization multiplexed images in three layers spaced by 40 µm, which were then read out using a charge coupled device (CCD) and a white light source (Supplementary Movie 1). This technique allows for one-shot readout of patterns, and when multiple CCDs are used it can provide instant and simultaneous readout of all recorded patterns. Additionally, the modulation of the transmission introduced by the patterns can be used as a polarization- and wavelength-dependent signal modulator for optical devices. For example, the large extinction of gold nanorods allows for customized modulation in multiple wavelength bands of a supercontinuum light source. This can be accomplished in a single (on chip) filter, which does not suffer from bleaching and exhibits a high damage threshold of >10 mJ cm^{-2} (based on the threshold energy required for recording a pixel).

Most importantly, the presented technique could be highly beneficial for high density optical data storage. As demonstrated in Fig. 4, incorporation of two polarization and three wavelength channels, a 10-µm spacer layer, and a bit spacing equal to the bit diameter of 0.75 µm amounts to a bit density of 1.1 Tbit cm^{-3}. This results in a disk capacity of 1.6 Tbyte for a DVD sized disk. We have performed recording and readout in ten layers (Supplementary Fig. 6), demonstrating the feasibility of our technology for application on a disk. Further improvement in data capacity is warranted if three-state polarization encoding (Supplementary Fig. 7) is combined with a thinner spacer. A threefold reduction in spacer layer thickness is feasible, considering the recording layer thickness of 1 µm, resulting in a disk capacity of 7.2 Tbyte. Our bit-by-bit recording technique is fully compatible with existing drive technology, and allows for recording speeds up to 1 Gbit s^{-1} when a high repetition rate laser source is used[28]. Owing to the low recording pulse energy (<0.5 nJ per pulse), a drastic increase in recording speed can be achieved when a supercontinuum light source is used for simultaneous recording in all channels.

METHODS SUMMARY

Sample preparation. Gold nanorods with average aspect ratios of 2.3 ± 1, 4.3 ± 1 and 6 ± 2 were prepared using wet chemical synthesis[29,30]. The nanorod solutions were then combined to obtain a 'flat' extinction profile in the 700–1,000 nm wavelength range. The nanorods were mixed with a 15 wt% polyvinyl alcohol solution, and spin-coated on a glass coverslip. The thickness of this layer was 1 ± 0.2 µm, measured using an atomic force microscope. The approximate nanorod concentration in the film was 400 ± 50 nM (~200 nanorods in the focal volume of the 0.95 NA objective lens). Subsequently, a transparent pressure-sensitive adhesive (LINTEC Co.) with a thickness of 10 ± 1 µm and a refractive index of 1.506 was laminated onto the spin-coated layer. This process was repeated until the desired number of layers was reached (for more details, see Supplementary Information).
Optical set-up. Both recording and readout were conducted in the same homebuilt microscope. For recording, an electro-optic modulator selected single pulses from the pulse train of a femtosecond pulse laser (SpectraPhysics Tsunami, 100 fs pulse duration, 82 MHz repetition rate, tunable between 690 and 1,010 nm). The laser pulses were focused onto the sample through a high NA objective lens (Olympus 0.95 NA 40×, coverslip corrected). For readout, the TPL of the nanorods was excited using the 82 MHz output from the femtosecond laser. The TPL signal was directed to a photomultiplier tube (Hamamatsu H7422P40) and was detected in the 400–600 nm wavelength range. To prevent erasure of the patterns, the pulse energy of the readout laser was almost three orders of magnitude lower than the patterning pulse energy (for more details see Supplementary Information).

1. Moerner, W. E. *Persistent Spectral Hole-Burning: Science and Applications* (Springer, 1988).
2. Ditlbacher, H., Krenn, J. R., Lamprecht, B., Leitner, A. & Aussenegg, F. R. Spectrally coded optical data storage by metal nanoparticles. *Opt. Lett.* **25**, 563–565 (2000).
3. Pham, H. H., Gourevich, I., Oh, J. K., Jonkman, J. E. N. & Kumacheva, E. A multidye nanostructured material for optical data storage and security data encryption. *Adv. Mater.* **16**, 516–520 (2004).
4. Alasfar, S. *et al.* Polarization-multiplexed optical memory with urethane-urea copolymers. *Appl. Opt.* **38**, 6201–6204 (1999).
5. Niidome, Y., Urakawa, S., Kawahara, M. & Yamada, S. Dichroism of poly(vinylalcohol) films containing gold nanorods induced by polarized pulsed-laser irradiation. *Jpn J. Appl. Phys.* **42**, 1749–1750 (2003).
6. Wilson, O., Wilson, G. J. & Mulvaney, P. Laser writing in polarized silver nanorod films. *Adv. Mater.* **14**, 1000–1004 (2002).
7. Pérez-Juste, J., Rodríguez-González, B., Mulvaney, P. & Liz-Marzán, L. M. Optical control and patterning of gold-nanorod-poly(vinyl alcohol) nanocomposite films. *Adv. Funct. Mater.* **15**, 1065–1071 (2005).
8. Li, X. P., Chon, J. W. M., Wu, S. H., Evans, R. A. & Gu, M. Rewritable polarization-encoded multilayer data storage in 2,5-dimethyl-4-(p-nitrophenylazo)anisole doped polymer. *Opt. Lett.* **32**, 277–279 (2007).
9. Strickler, J. & Webb, W. Three-dimensional optical data storage in refractive media by two-photon point excitation. *Opt. Lett.* **16**, 1780–1782 (1991).
10. Heanue, J. F., Bashaw, M. C. & Hesselink, L. Volume holographic storage and retrieval of digital data. *Science* **265**, 749–752 (1994).
11. Cumpston, B. H. *et al.* Two-photon polymerization initiators for three-dimensional optical data storage and microfabrication. *Nature* **398**, 51–54 (1999).
12. Kawata, S. & Kawata, Y. Three-dimensional optical data storage using photochromic materials. *Chem. Rev.* **100**, 1777–1788 (2000).
13. Day, D., Gu, M. & Smallridge, A. Rewritable 3D bit optical data storage in a PMMA-based photorefractive polymer. *Adv. Mater.* **13**, 1005–1007 (2001).
14. Novo, C. *et al.* Contributions from radiation damping and surface scattering to the linewidth of the longitudinal plasmon band of gold nanorods: a single particle study. *Phys. Chem. Chem. Phys.* **8**, 3540–3546 (2006).
15. Sönnichsen, C. *et al.* Drastic reduction of plasmon damping in gold nanorods. *Phys. Rev. Lett.* **88**, 077402 (2002).
16. Chang, S. S., Shih, C. W., Chen, C. D., Lai, W. C. & Wang, C. R. C. The shape transition of gold nanorods. *Langmuir* **15**, 701–709 (1999).
17. Link, S., Burda, C., Nikoobakht, B. & El-Sayed, M. A. Laser-induced shape changes of colloidal gold nanorods using femtosecond and nanosecond laser pulses. *J. Phys. Chem. B* **104**, 6152–6163 (2000).
18. Habenicht, A., Olapinski, M., Burmeister, F., Leiderer, P. & Boneberg, J. Jumping nanodroplets. *Science* **309**, 2043–2045 (2005).
19. Chon, J. W. M., Bullen, C., Zijlstra, P. & Gu, M. Spectral encoding on gold nanorods doped in a silica sol-gel matrix and its application to high density optical data storage. *Adv. Funct. Mater.* **17**, 875–880 (2007).
20. Zijlstra, P., Chon, J. W. M. & Gu, M. Effect of heat accumulation on the dynamic range of a gold nanorod doped nanocomposite for optical laser writing and patterning. *Opt. Express* **15**, 12151–12160 (2007).
21. Wang, H. F. *et al.* In vitro and in vivo two-photon luminescence imaging of single gold nanorods. *Proc. Natl Acad. Sci. USA* **102**, 15752–15756 (2005).
22. Bouhelier, A. *et al.* Surface plasmon characteristics of tunable photoluminescence in single gold nanorods. *Phys. Rev. Lett.* **95**, 267405 (2005).
23. Xu, C. & Webb, W. W. Measurement of two-photon excitation cross sections of molecular fluorophores with data from 690 to 1050 nm. *J. Opt. Soc. Am. B* **13**, 481–491 (1996).
24. Mohamed, M. B., Volkov, V., Link, S. & El-Sayed, M. A. The 'lightning' gold nanorods: fluorescence enhancement of over a million compared to the gold metal. *Chem. Phys. Lett.* **317**, 517–523 (2000).
25. Dulkeith, E. *et al.* Plasmon emission in photoexcited gold nanoparticles. *Phys. Rev. B* **70**, 205424 (2004).
26. Ramakrishna, G., Varnavski, O., Kim, J., Lee, D. & Goodson, T. Quantum sized gold clusters as efficient two photon absorbers. *J. Am. Chem. Soc.* **130**, 5032–5033 (2008).
27. Mooradian, A. Photoluminescence of metals. *Phys. Rev. Lett.* **22**, 185–187 (1969).
28. Tanaka, T. & Kawata, S. Three-dimensional multi-layered fluorescent optical disk. In *Technical Digest Int. Symp. Opt. Mem.* Tu-G-01 (Adthree Publishing, Tokyo, 2007).
29. Nikoobakht, B. & El-Sayed, M. A. Preparation and growth mechanism of gold nanorods (NRs) using seed-mediated growth method. *Chem. Mater.* **15**, 1957–1962 (2003).
30. Zijlstra, P., Bullen, C., Chon, J. W. M. & Gu, M. High-temperature seedless synthesis of gold nanorods. *J. Phys. Chem. B* **110**, 19315–19318 (2006).

Author Information Reprints and permissions information is available at www.nature.com/reprints. Correspondence and requests for materials should be addressed to J.W.M.C. (JChon@groupwise.swin.edu.au).